

QUANTITATIVE CONTRIBUTION OF CYP2D6 AND CYP3A TO OXYCODONE METABOLISM IN HUMAN LIVER AND INTESTINAL MICROSOMES

Bojan Lalovic, Brian Phillips, Linda L. Risler, William Howald, and Danny D. Shen

Departments of Pharmaceutics (B.L., D.D.S.), Medicinal Chemistry (W.H.), and Pharmacy (D.D.S.), University of Washington; and Clinical Research Division, Fred Hutchinson Cancer Research Center (B.L., B.P., L.L.R., D.D.S.), Seattle, Washington

(Received July 17, 2003; accepted December 29, 2003)

This article is available online at <http://dmd.aspetjournals.org>

ABSTRACT:

Oxycodone undergoes *N*-demethylation to noroxycodone and *O*-demethylation to oxymorphone. The cytochrome P450 (P450) isoforms capable of mediating the oxidation of oxycodone to oxymorphone and noroxycodone were identified using a panel of recombinant human P450s. CYP3A4 and CYP3A5 displayed the highest activity for oxycodone *N*-demethylation; intrinsic clearance for CYP3A5 was slightly higher than that for CYP3A4. CYP2D6 had the highest activity for *O*-demethylation. Multienzyme, Michaelis-Menten kinetics were observed for both oxidative reactions in microsomes prepared from five human livers. Inhibition with ketoconazole showed that CYP3A is the high affinity enzyme for oxycodone *N*-demethylation; ketoconazole inhibited >90% of noroxycodone formation at low substrate concentrations. CYP3A-mediated noroxycodone formation exhibited a mean K_m of $600 \pm 119 \mu\text{M}$ and a V_{max} that ranged from 716 to 14523 pmol/mg/min.

Contribution from the low affinity enzyme(s) did not exceed 8% of total intrinsic clearance for *N*-demethylation. Quinidine inhibition showed that CYP2D6 is the high affinity enzyme for *O*-demethylation with a mean K_m of $130 \pm 33 \mu\text{M}$ and a V_{max} that ranged from 89 to 356 pmol/mg/min. Activity of the low affinity enzyme(s) accounted for 10 to 26% of total intrinsic clearance for *O*-demethylation. On average, the total intrinsic clearance for noroxycodone formation was 8 times greater than that for oxymorphone formation across the five liver microsomal preparations (10.5 $\mu\text{l/min/mg}$ versus 1.5 $\mu\text{l/min/mg}$). Experiments with human intestinal mucosal microsomes indicated lower *N*-demethylation activity (20–50%) compared with liver microsomes and negligible *O*-demethylation activity, which predict a minimal contribution of intestinal mucosa in the first-pass oxidative metabolism of oxycodone.

Oxycodone (4,5-epoxy-14-hydroxy-3-methoxy-17-methylmorphinan-6-one; 14-dihydrohydroxycodone) is an opioid analgesic widely used for the treatment of postoperative pain (Nuutinen et al., 1986; Silvasti et al., 1998; Curtis et al., 1999) and pain associated with cancer (De Conno et al., 1991; Glare and Walsh, 1993; Parris et al., 1998). It has also been suggested for the management of nonmalignant chronic pain (Watson and Babul, 1998; Sindrup and Jensen, 1999).

Oxycodone is extensively metabolized; only 10% of dose is excreted unchanged in urine (Poyhia et al., 1991; Kirvela et al., 1996). The known metabolic scheme of oxycodone is presented in Fig. 1. Oxymorphone, a 3-*O*-demethylation metabolite of oxycodone, is a potent opioid that has a 3 to 5 times higher μ -opioid receptor affinity than morphine (Childers et al., 1979; Chen et al., 1991). Oral oxymorphone is 10-fold more potent than oral morphine based on dose (Melmon et al., 2000).

Cytochrome P450 (P450¹) enzyme CYP2D6 is known to catalyze

Supported in part by National Institutes of Health Grant AT00864. B.L. is a recipient of the National Institutes of Health Pharmaceutical Sciences Training Grant (GM07750).

¹ Abbreviations used are: P450, cytochrome P450; NOC, noroxycodone; OM, oxymorphone; HLM, human liver microsomes; LC-MS, liquid chromatography-mass spectrometry; PM, poor metabolizer.

Address correspondence to: Dr. Danny D. Shen, Department of Pharmacy, University of Washington, Box 357630, Seattle, WA 98105. E-mail: ds@u.washington.edu

the *O*-demethylation of 3-methoxy-17-methyl morphinans, e.g., codeine, to morphine (Dayer et al., 1988) and dextromethorphan to dextrorphan (Kronbach et al., 1987; Dayer et al., 1989). Morphine derived from the oxidation of codeine has been shown to account for most, if not all, of the analgesic activity of codeine (Caraco et al., 1996a; Poulsen et al., 1996). Until recently, oxycodone *O*-demethylation to oxymorphone was thought to be a CYP2D6-mediated bioactivation process, similar to codeine. Otton et al. (1993) demonstrated that CYP2D6 is the principal *O*-demethylase; oxymorphone formation in human liver microsomes was much lower in CYP2D6 poor metabolizers, as compared with extensive metabolizers, and inhibited by quinidine, a selective CYP2D6. Also, Somogyi (1999) has reported that oxymorphone formation in human liver microsomes was inhibited by anti-CYP2D6. However, blockade of oxymorphone formation by quinine has been shown not to decrease the antinociceptive effect of oxycodone in rats (Cleary et al., 1994). Inhibition of CYP2D6 by quinidine did not attenuate the opioid-induced side effects of oxycodone in human volunteers (Kaiko et al., 1996; Heiskanen et al., 1998).

Oxycodone also undergoes *N*-demethylation at the 17-position to noroxycodone (Weinstein and Gaylord, 1979; Somogyi, 1999). CYP3A4 is known to catalyze the *N*-demethylation of codeine (Gorski et al., 1994) and dextromethorphan (Caraco et al., 1996b), but the role of this enzyme in the *N*-demethylation of oxycodone has not been established. Leow and Smith (1994) reported that noroxycodone exhibited modest analgesic potency after i.c.v. administration in the rat.

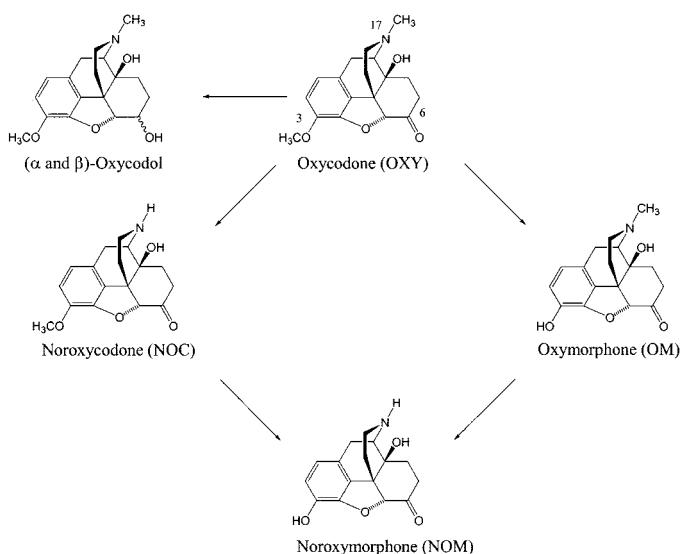


FIG. 1. Oxycodone metabolic scheme.

Noroxycodone or its metabolites may be a source of active metabolites that play a role in the analgesia of oxycodone. Other metabolic pathways involving 6-keto reduction and conjugation of oxycodone have been identified in animals (Ishida et al., 1979, 1982) but have not been assessed in humans.

We have conducted *in vitro* metabolic studies to identify the specific P450s involved in the oxidation of oxycodone and to assess their respective contribution toward the intrinsic metabolic clearance of each pathway. The ability of a panel of recombinant human P450s to *O*- and *N*-demethylate oxycodone was examined. This was followed by studies in human liver and intestinal microsomes to 1) fully characterize the Michaelis-Menten kinetics of noroxycodone and oxymorphone formation, and 2) assess the contribution of the identified P450 isoform(s) through incubation studies with P450-specific inhibitors.

Materials and Methods

Materials. Oxycodone hydrochloride, quinidine, and NADPH were purchased from Sigma-Aldrich (St. Louis, MO). Ketoconazole was obtained from Research Diagnostics (Flanders, NJ). A BCA Protein Assay Kit was purchased from Pierce Chemical (Rockford, IL). Standard solutions of oxycodone, noroxycodone (NOC), oxymorphone (OM), and their deuterated analogs d^3 -NOC and d^3 -OM (labeled at the 17- or the 3-methyl hydrogens, respectively) in methanol were purchased from Cerilliant Inc. (Austin, TX). All chemicals and solvents used were of the highest chemical grade available.

Microsomes containing individual recombinant human cytochrome P450 isoforms expressed in either lymphoblastoid (1A1, 1A2, 2A6, 2B6, 2C8, 2C9*1, 2C19, 2D6*1, 2E1, 3A4) or SF9 insect cells (Supersomes) (2D6*1, 3A4, and 3A5) were purchased from BD Gentest (Woburn, MA). Human cytochrome *b*₅ was obtained from PanVera Corp. (Madison, WI). Pooled human liver microsomes (lot H0610) were purchased from Xenotech, LLC (Kansas City, KS). The manufacturers provided the microsomal protein concentration data.

Preparation of Human Liver Microsomes. Human livers HL141, 146, 148, and 153, and homogenates of mucosa from human intestine HI 20, 21, 29, 35, and 40 (jejunal, duodenal, and ileal sections) were obtained from the University of Washington School of Pharmacy Human Tissue Bank. The University of Washington Human Subjects Review Board approved the use of human donor tissues for research purposes. Microsomes were prepared from each liver (HLM) and intestine according to previously described methods (Gibbs et al., 1999; Madani et al., 1999). The selected livers represented the range of CYP2D6 and CYP3A activity across the liver bank, since these enzymes were most likely to be involved in oxycodone metabolism. The

selected HLMs were not deficient in other P450 activities. The microsomes were stored at -80°C until use. Final determinations of protein concentration were performed using the Pierce Protein Assay Kit with bovine serum albumin as standard.

Microsomal Incubations. Incubations were conducted in 2-ml Eppendorf screw-top plastic tubes. The 0.5-ml incubates contained 0.1 to 0.2 mg/ml microsomal protein, 0.1 to 800 μM oxycodone, and 1 mM NADPH in 100 mM, pH 7.4 phosphate buffer. The substrate was added to the microsomal suspension, and the oxidative reactions were started with the addition of NADPH after a 5-min preequilibration period. All incubations were performed in duplicate, in a 37°C water bath-shaker over time intervals varying from 0 to 30 min. The inhibitors, ketoconazole and quinidine, were dissolved in an 80:20 (v/v) mix of methanol:water. An aliquot of the inhibitor was placed in the incubation tubes and the solution was evaporated to dryness under N_2 for 15 min. Addition of other components of the incubation mixture followed. Metabolic reactions were terminated by protein precipitation with the addition of 1 ml of ice-cold acetonitrile. The tubes were immediately vortexed for 2 to 3 s and immersed in ice. At a later time, internal standards d^3 -NOC and d^3 -OM were added at 20 ng each. Samples were then spun in a microcentrifuge at 16,000g for 5 min to pellet the protein. The supernatant was collected and dried under N_2 in a fresh tube. The samples were reconstituted in 150 μl of mobile phase, of which 1 to 5 μl was injected onto the liquid chromatograph-mass spectrometer for metabolite analysis.

Metabolite Analysis. Oxycodone metabolites in human liver microsomes were analyzed by liquid chromatography-mass spectrometry (LC-MS). Chromatographic separation of the analytes was achieved with a 5- μm , 2.1 mm \times 150 mm Zorbax SSB C18 column (Agilent Technologies, Palo Alto, CA). The mobile phase consisted of an 88:12 (v/v) mix of 10 mM, pH 4 potassium acetate and acetonitrile. The flow rate was set at 0.25 ml/min. Oxymorphone eluted at 3 min and noroxycodone at 6 min. Oxycodone eluted at 7 to 8 min. The retention times of the d^3 -internal standards did not differ from the proteoanalyses.

The mass spectrometer was operated in the atmospheric pressure ionization electrospray mode with positive polarity. The m/z 340 $[\text{M} + \text{K}]^+$ ion was monitored for oxymorphone and the m/z 302 $[\text{M} + \text{H}]^+$ ion for noroxycodone; m/z 343 $[\text{M} + \text{K}]^+$ and m/z 305 $[\text{M} + \text{H}]^+$ were monitored for the respective deuterated internal standard analogs. The molecular ion for oxycodone was not routinely monitored.

Calibration standards and quality controls were prepared in heat-inactivated human liver microsomal suspensions at protein concentrations used in the kinetic experiments (0.2 mg/ml). Peak area ratios of oxymorphone to oxymorphone- d^3 were linear over the range of 0.1 to 150 ng when the $[\text{M} + \text{K}]^+$ ion was monitored. For noroxycodone, the linear range was 0.25 to 1000 ng when the $[\text{M} + \text{H}]^+$ molecular ion was monitored. Limits of quantification were 0.1 ng per 0.5 ml (0.2 ng/ml) of microsomal incubates for oxymorphone, and 0.25 ng per 0.5 ml (0.5 ng/ml) of incubate for noroxycodone. The intraday (within-batch) accuracy and precision of the LC-MS assay was determined by replicate assay of spiked microsomal samples ($n = 15$) at three different concentration levels corresponding to low, intermediate, and high regions of the calibration range; i.e., 6.6, 75, or 125 ng of oxymorphone and 26.6, 250, or 750 ng of noroxycodone. Interday quality control data were obtained by assaying the same spiked samples in duplicate over 5 nonconsecutive days. The *interday* and *intraday* mean values were not significantly different from each other. Their coefficients of variation were well less than 10%.

Initial analysis revealed a trace, contaminating presence of oxymorphone and noroxycodone in the commercial supply of oxycodone. The percentage of each contaminating compound was determined and applied as a correction factor for both the calibration standards and the incubate samples. For the calibration standards, the correction being constant was 0.1% for noroxycodone and 0.01% oxymorphone. For the incubate samples, the extent of correction was variable and depended on the nominal substrate (oxycodone) concentration and the amount of metabolite formed. The maximum correction was 15% of the observed amount of noroxycodone formed, and 1 to 2% of the amount of oxymorphone formed.

Optimization of Incubation Condition. To establish the optimal condition for initial velocity measurement, we determined the linearity of noroxycodone and oxymorphone formation with respect to time (0.5–40 min) and microsomal protein concentration (0.1–5 mg/ml) at various substrate concentrations.

Additionally, a mass-balance study was performed to examine whether the loss of oxycodone during the incubation period could be accounted for by the formation of oxymorphone and noroxycodone, i.e., to rule out the presence of any unrecognized, competing metabolic processes. Oxycodone at 2 μM was incubated in triplicates over 0, 30, 60, 90, and 120 min in Xenotech liver microsomes. Oxycodone depletion was measured as the difference between the oxycodone concentration observed at the incubation stop-times and the initial oxycodone concentration.

cDNA-Expressed P450. To identify which human P450 isoforms mediate the formation of noroxycodone and oxymorphone, oxycodone was incubated with a panel of human lymphoblastoid microsomes expressing individual human P450 enzymes. Incubations were performed with microsomes expressing 1A1, 1A2, 2A6, 2B6, 2C8, 2C9, 2C19, 2D6, 2E1, and 3A4. No oxycodone turnover was observed in control incubations performed with microsomes transfected with expression vector alone. Reactions were carried out at 5, 15, and 150 μM oxycodone, using the procedure outlined in the preceding section. The concentration of microsomal protein used in these experiments was as recommended by the manufacturer. Additional P450 metabolic screening was conducted with noroxycodone and oxymorphone as substrates to examine formation of the common di-demethylated secondary metabolite noroxymorphone.

To further define the saturation kinetics of oxymorphone and noroxycodone formation from oxycodone, as well as noroxymorphone from either oxymorphone or noroxycodone, incubations were performed over the substrate range of 1 to 750 μM in Supersomes expressing CYP3A4, 3A5, and 2D6*1, either with or without supplementation of cytochrome b_5 (i.e., at 3:1 molar ratio of cytochrome b_5 to P450).

Noroxycodone and Oxymorphone Formation Kinetics. Initial velocities of noroxycodone and oxymorphone formation were determined at 15 concentrations of oxycodone that ranged from 0.1 to 800 μM . Parallel sets of incubations at 10, 30, 100, 300, 650, or 800 μM oxycodone were performed in the presence of 20, 60, or 200 nM quinidine (CYP2D6 inhibitor) or ketoconazole (CYP3A inhibitor). The chosen inhibitor concentrations ranged from 1 to 10 times the known K_i , whereas the substrate concentrations ranged from below to above the oxycodone K_m (Otton et al., 1993; Gibbs et al., 1999).

For each preparation of human liver microsomes, formation velocity data for noroxycodone and oxymorphone in the presence and absence of an inhibitor were fitted to either a one- (eq. 1) or two-enzyme model (eqs. 2 and 3). The two-enzyme models consisted of either two saturable (Michaelis-Menten) components (eq. 2) or a single saturable (MM) component and a second, linear component (eq. 3).

$$v = \frac{V_{\max 1} \cdot S}{K_{m1} + S} \quad (1)$$

$$v = \frac{V_{\max 1} \cdot S}{K_{m1} + S} + \frac{V_{\max 2} \cdot S}{K_{m2} + S} \quad (2)$$

$$v = \frac{V_{\max 1} \cdot S}{K_{m1} + S} + E_2 \cdot S \quad (3)$$

v represents the metabolite formation velocity, K_{m1} the Michaelis-Menten constant of the substrate for the high affinity enzyme, $V_{\max 1}$ the maximum formation velocity for the high affinity enzyme, S the substrate concentration, and E_2 the V/K ratio for the high or low affinity enzyme.

Three simple inhibition models, i.e., competitive, noncompetitive, and uncompetitive inhibition, were considered for the effects of quinidine and ketoconazole as defined in the equations below (Segel, 1975), with K_i as the dissociation constant of the inhibitor-enzyme complex and I the inhibitor concentration. Metabolite formation velocity data from control incubations and incubations with inhibitor were fitted simultaneously to the model equations.

$$\text{Competitive Inhibition } K_{m1} = K_{m1} \cdot \left(1 + \frac{I}{K_i}\right) \quad (4)$$

$$\text{Noncompetitive Inhibition } V_{\max 1} = \frac{V_{\max 1}}{\left(1 + \frac{I}{K_i}\right)} \quad (5)$$

$$\text{Uncompetitive Inhibition } V_{\max 1} = \frac{V_{\max 1}}{\left(1 + \frac{I}{K_i}\right)} \quad K_{m1} = \frac{K_{m1}}{\left(1 + \frac{I}{K_i}\right)} \quad (6)$$

Ketoconazole and quinidine were assumed to inhibit the high affinity component of each oxidative reaction. Nonlinear regression fit of data to the model equations was performed using the numeric module of SAAM II (Version 1.1; University of Washington, Seattle, WA). A fractional standard deviation error model (10%) was applied to the fits based on known analytical errors.

The choice of enzyme models was judged by the F -ratio test (unweighted residual sum of squares), the Akaike information criterion value, plots of residuals, visual inspection of the model fit, and the 95% confidence intervals of the parameter estimates.

Oxycodone oxidation by microsomes isolated from the intestinal mucosa was examined at a single substrate concentration (10 μM). A parallel set of incubations was performed with fixed single inhibitor concentrations of quinidine and ketoconazole (100 nM) to assess the involvement of CYP3A and 2D6 in the intestinal metabolism of oxycodone.

Microsomal Protein Binding. To determine the extent to which oxycodone binds to human liver microsomes, we performed equilibrium dialysis studies using a Spectra/Por Equilibrium Dialyzer (Spectrum Laboratories Inc., Rancho Dominguez, CA) equipped with microcells (0.5 ml/cell). Regenerated cellulose membrane discs with a 12- to 14-kDa cutoff (Spectrum Laboratories Inc.) were rinsed in distilled water and soaked in 100 mM, pH 7.4 phosphate buffer prior to use. Microsomal suspensions (0.2 mg/ml of protein) spiked with oxycodone were dialyzed against in 100 mM, pH 7.4 phosphate buffer. The experiments were conducted at two substrate concentrations, 7 and 70 μM , over 3 and 6 h. The microsomal free fraction was expressed as the ratio of buffer side (free) concentration divided by the protein side (total) concentration. The dialysates were assayed according to the LC-MS method described above.

Results

Linearity of Metabolite Formation and Mass Balance. To establish the appropriate microsomal incubation conditions for initial velocity measurements, linearity of metabolite formation was observed over a 40-min incubation period and over a protein concentration range of 0.1 to 5 mg/ml, independent of substrate concentration. Negligible loss of oxycodone or formation of metabolites was detected in control incubations without the addition of NADPH.

A mass-balance experiment was performed to determine whether the N - and O - demethylation reactions quantitatively account for the metabolic loss of oxycodone. Substrate consumption was <5% over the first 30 min, increasing to 20% by 120 min. Figure 3 shows that loss of oxycodone over the 2-h incubation was reasonably accounted for by the formation of oxymorphone and noroxycodone, and no apparent competing oxidative processes were observed. Although the secondary metabolite noroxymorphone was not quantitated, it may account for the small differences between parent loss and primary metabolite formation observed at 90 and 120 min.

cDNA-Expressed Human P450s. A set of lymphoblastoid microsomes expressing individual P450 enzyme was used to examine which human drug-metabolizing P450 isoforms are capable of transforming oxycodone to noroxycodone and oxymorphone. Figure 2 shows the oxidative activity of individual P450s in forming noroxycodone and oxymorphone at 15, 150, and 500 μM oxycodone. The formation velocity is normalized by P450 content of each microsomal preparation. CYP3A4 showed the highest specific activity for conversion of oxycodone to noroxycodone (Fig. 2, left panel); noroxycodone formation was readily measurable at the lowest substrate concentration of 15 μM . Several other P450s including 2A6, 2C9, and 2C19 mediated oxycodone N -demethylation as well, but were only measurable at the highest substrate concentration of 500 μM . N -Demethylation was notably absent with CYP2D6. O -Demethylation of oxyc-

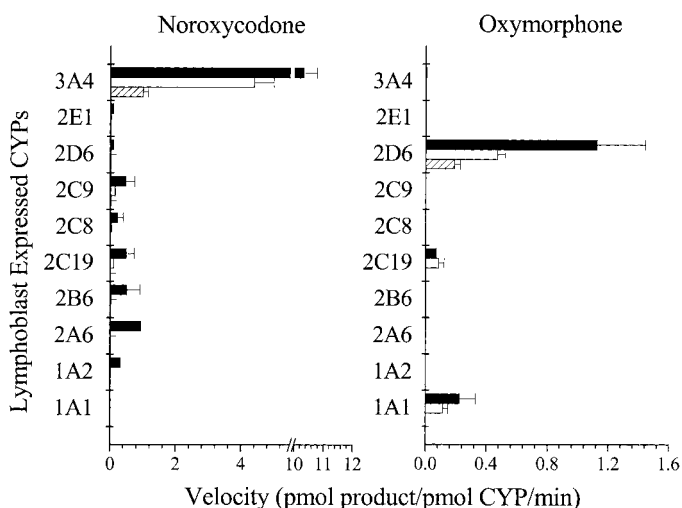


Fig. 2. Noroxycodone (NOC) and oxymorphone (OM) formation (per pmol of P450) in lymphoblast microsomes expressing individual cDNA-expressed human P450s.

The experiment was performed at three oxycodone concentrations: 15 (▨), 150 (□), and 500 (■) μ M.

oxycodone to oxymorphone (Fig. 2, right panel) was the highest with CYP2D6. Aside from this, only 2C19 and 1A1 (an intestinal P450) showed barely detectable activities at the highest substrate concentration.

This panel of recombinant P450s was also used to examine the convergent, secondary metabolism of oxymorphone and noroxycodone to noroxymorphone. CYP2D6 catalyzed *O*-demethylation of noroxycodone to noroxymorphone exclusively and was readily measurable at all three substrate concentrations (data not shown). Only negligible *N*-demethylation of oxymorphone to noroxymorphone was observed with both CYP2D6 and CYP3A4, and was only measurable at the highest substrate concentration of 500 μ M and at rates that are 20- to 30-fold lower compared with noroxycodone *O*-demethylation.

Noroxycodone Formation in Human Liver Microsomes. Preliminary Eadie-Hofstee analysis of noroxycodone formation velocity versus substrate concentration data indicated two distinct kinetic phases with several of the human liver microsomal preparations. To better resolve the multienzyme kinetics and ascertain which kinetic component reflects CYP3A-mediated oxidation, we extended our kinetic experiments to include incubations with ketoconazole, a CYP3A-selective inhibitor.

Figure 4 shows representative saturation profiles of noroxycodone formation and the effect of ketoconazole obtained in two microsomal preparations, which illustrate different kinetic behavior between livers. HLM 141 data exhibited multienzyme kinetics, whereas HLM 148 data followed uni-enzyme kinetics. The distinction was most evident when their Dixon plots were compared; i.e., curvilinear Dixon plot for HLM 141 in contrast to a clearly linear Dixon plot for HLM 148. Greater than 90% inhibition of *N*-demethylation activity was consistently achieved at the highest ketoconazole concentration of 200 nM in microsomes from all five human donor livers, which reflect the dominant role of CYP3A in the formation of noroxycodone. This is consistent with the earlier experiments with cDNA-expressed P450s.

Noroxycodone formation velocity data from individual human liver microsomes were fit to either a single-enzyme Michaelis-Menten equation (eq. 1) or a two-enzyme model consisting of a saturable, Michaelis-Menten component and a linear, low affinity term (eq. 3). Attempts to fit the data to more complex models, the two-enzyme Michaelis-Menten model (eq. 2) or three-enzyme models, either failed to converge or

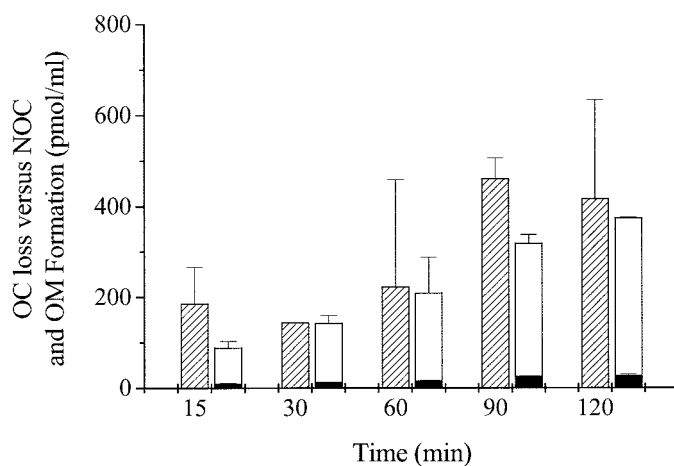


Fig. 3. Oxycodone (▨) loss compared with the amount of oxidative metabolites, noroxycodone (□) and oxymorphone (■) formed over a 2-h incubation period in the presence of NADPH.

The bars represent mean and S.D. of triplicate determinations. Oxymorphone values are stacked against noroxycodone values.

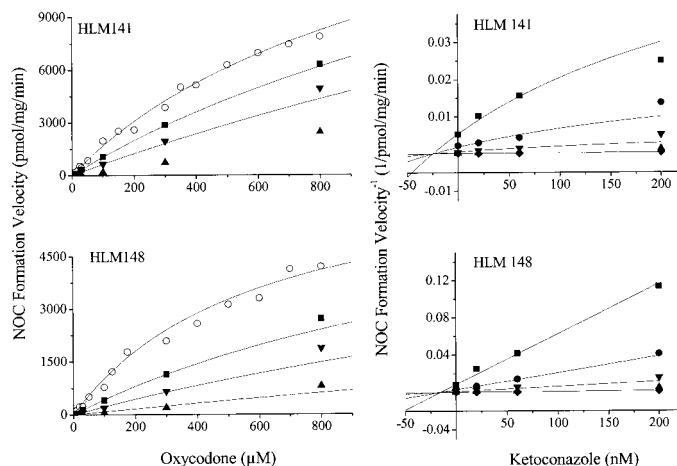


Fig. 4. Noroxycodone formation kinetics (left panels) in HLM 141 (top) and 148 (bottom) over an oxycodone concentration range of 0.1 to 800 μ M in the absence (○) and presence of ketoconazole at 20 (■), 60 (▼), and 200 (▲) nM.

Right panels represent the corresponding Dixon plots of data at substrate concentrations of 10 (■), 30 (●), 100 (▼), 300 (▲), and 850 (◆) μ M. Solid lines represent model predictions. Velocity data from HLM 141 were fit to a two-enzyme model (curved Dixon), whereas HLM 148 data were fit to a one-enzyme model (linear Dixon).

yielded poorer fits. The single-enzyme Michaelis-Menten model best described noroxycodone formation in Xenotech, HLM 148, and HLM 153 microsomes. The two-enzyme model (eq. 3) was best for HLM 141 and HLM 146. Estimates of noroxycodone kinetic parameters for each of the five human liver microsomal preparations are presented in Table 1. The competitive model was consistently superior to the noncompetitive and uncompetitive models in describing the inhibition kinetics of ketoconazole for all five liver preparations.

Data modeling confirmed CYP3A as the high affinity enzyme for noroxycodone formation. As indicated above, a low affinity, non-CYP3A-related component was identifiable in HLM 141 and HLM 146. Even in those two livers, the contribution of low affinity enzyme(s) in the overall formation velocity at low substrate concentration ($\ll K_{m1}$) was minor; intrinsic clearance due to the low affinity component (E_2) accounted for merely 7 to 8% of the total intrinsic clearance ($E_1 + E_2$) of the *N*-demethylation pathway.

TABLE 1

Estimates of Michaelis-Menten parameters for noroxycodone formation and the competitive K_i for ketoconazole

Values in parentheses represent the 95% confidence intervals of the regression estimates.

| Liver Microsomes | K_{m1} | V_{max1} | E_1^a | E_2 | K_i | CYP3A4 Content ^b | CYP3A5 Content ^b |
|------------------|-------------------|------------------------------------|------------------------------------|---------------------|---------------------|-----------------------------|-----------------------------|
| | μM | $\text{pmol}/\text{mg}/\text{min}$ | $\mu\text{L}/\text{mg}/\text{min}$ | | nM | | pmol/mg |
| Xenotech | 524 (369–680) | 6071 (4525–7618) | 11.6 | | 17.9 (14.8–21.1) | | |
| HLM141 | 804 (517–1090) | 14,523 (9536–19,510) | 18.1 | 1.41 (0.02–2.6) | 25.1 (17.3–33.0) | 70.6 | 372 |
| HLM146 | 506 (155–857) | 716 (325–1107) | 1.2 | 0.09 (0.02–0.17) | 17.5 (6.5–28.5) | 10 | N.D. |
| HLM148 | 571 (389–753) | 7174 (5251–9098) | 12.6 | | 15.4 (12.9–18.0) | 133 | 2.3 |
| HLM153 | 597 (347–848) | 4403 (2890–5915) | 7.4 | | 28.0 (19.8–36.2) | 41.3 | 3.0 |
| Mean \pm S.D. | 600 ± 119 | 6577 ± 5070 | 10.2 ± 6.3 | 0.7 ± 0.9 | 20.8 ± 5.5 | | |

N.D., not detected.

^a $E_1 = V_{max1}/K_{m1}$.

^b Data were previously reported by Lin et al. (2002).

A mean K_{m1} estimate of $600 \pm 119 \mu\text{M}$ was observed for CYP3A-mediated oxycodone *N*-demethylation in the five liver microsomal preparations (see Table 1), along with a large, 2.5-fold interliver variation in the V_{max1} . To investigate the reason for the large interliver variability in CYP3A-mediated noroxycodone formation, the content of CYP3A4 and CYP3A5 (picomoles of P450 per milligram of protein) was determined by Western blotting. The CYP3A4 and CYP3A5 content varied widely in our panel of human liver microsomes (see Table 1). Although CYP3A4 and CYP3A5 varied somewhat in parallel, the ratio of their content differed remarkably between microsomal preparations. HLM 146 contained little CYP3A5. HLM 141, on the other hand, displayed unusually high CYP3A5 content, 3-fold higher than its CYP3A4 content. The other two livers, HLM 148 and 153, contained CYP3A5 at levels lower than that of CYP3A4. The rank order of V_{max1} and E_1 estimates corresponded well with that of total CYP3A content, i.e., CYP3A4 plus CYP3A5.

The competitive K_i estimates of ketoconazole for CYP3A ranged between 15 and 28 nM, in agreement with published data (Gibbs et al., 1999). The presence of ketoconazole had no significant effect on oxymorphone formation, which is consistent with the absence of *O*-demethylation when oxycodone was incubated with cDNA-expressed CYP3A4.

In human intestinal microsomes, noroxycodone formation rate per milligram of protein at $10 \mu\text{M}$ oxycodone was 2- to 5-fold lower than in hepatic microsomes (data not shown). Noroxycodone formation was inhibited by 60 to 80% upon addition of 100 nM ketoconazole.

Oxymorphone Formation in Human Liver Microsomes. Initial analysis of the oxymorphone formation kinetics also suggested the involvement of at least two enzymes. To investigate whether CYP2D6 is the high affinity *O*-demethylase, the effect of quinidine was examined. Figure 5 shows representative saturation plots of oxymorphone formation in two human liver microsomes. All of the formation velocity versus substrate concentration plots failed to display a definite saturation plateau. For all five microsomal preparations, data were well described by a two-enzyme model consisting of a Michaelis-Menten and a linear term (eq. 3), along with competitive inhibition by quinidine (eq. 4). The model parameter estimates for the five human liver microsomal preparations are listed in Table 2. The mean K_{m1} estimate for CYP2D6 was $130 \pm 33 \mu\text{M}$; *O*-demethylation V_{max1} varied by 4-fold across the five liver preparations. The low affinity, non-CYP2D6 component (E_2) accounted for 11% to 26% of total intrinsic clearance ($E_1 + E_2$). The significant presence of a non-CYP2D6 component in the formation of oxymorphone is also reflected in the pronounced curvilinear Dixon plots as shown in Fig. 5 (right panel).

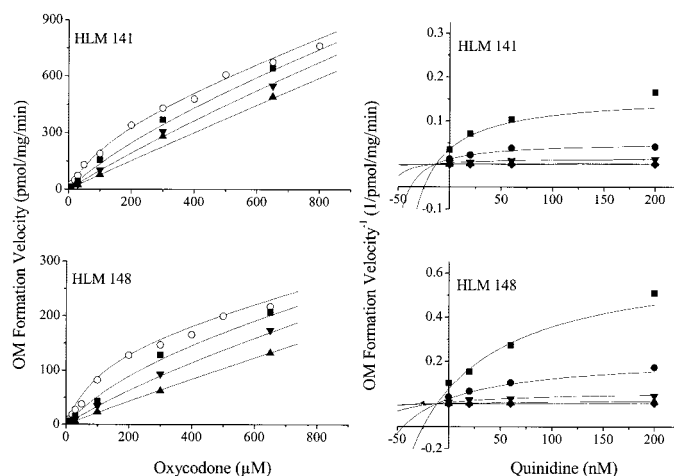


Fig. 5. Oxymorphone formation kinetics (left panels) in HLM 141 (top) and 148 (bottom) over an oxycodone concentration range of 0.1 to 800 μM in the absence (\circ) and presence of quinidine at 20 (\blacksquare), 60 (\blacktriangledown), and 200 (\blacktriangle) nM.

Right panels represent the corresponding Dixon plots of data at substrate concentrations of 10 (\blacksquare), 30 (\bullet), 100 (\blacktriangledown), 300 (\blacktriangle), and 650 (\blacklozenge) μM . Solid lines represent model predictions.

The mean K_i of quinidine on CYP2D6-mediated *O*-demethylation of oxycodone was $13 \pm 8 \text{ nM}$, which is within the range of reported K_i values of quinidine on CYP2D6-mediated oxidation of other substrates.

In human intestinal microsomes, oxymorphone formation rate at $10 \mu\text{M}$ oxycodone was at least 10- to 20-fold lower than in hepatic microsomes per milligram of protein; at 100 nM quinidine, no oxymorphone formation was detected.

Microsomal Protein Binding. Nonspecific binding of drug substrates in microsomal incubates restricts their access to the enzymes. Hence, correction of in vitro intrinsic metabolic clearance (V_{max}/K_m) for nonspecific binding is recommended, particularly when the in vitro clearance estimates are scaled to predict in vivo organ clearances (Obach, 1999). To determine whether oxycodone binds to the microsomal matrix, equilibrium dialysis experiments were performed on two of the microsomal preparations, HLM 148 and 153. These microsomal preparations exhibited negligible oxycodone binding at substrate concentrations of 7 and 70 μM .

Kinetic Studies with Supersome CYP3A4, CYP3A5, and CYP2D6. To compare the activities of CYP3A4 and CYP3A5 in noroxycodone formation, saturation kinetics of oxycodone *N*-demethylation were determined using Supersomes recombinant human

TABLE 2

Estimates of Michaelis-Menten parameters for oxymorphone formation and the competitive K_i for quinidine.

Values in parentheses represent the 95% confidence intervals of the regression estimates.

| Liver Microsomes | K_{m1} | V_{max1} | E_1^a | E_2 | K_i | CYP2D6 Content ^b |
|------------------|------------------|------------------|---------------|---------------------|---------------------|-----------------------------|
| | μM | $pmol/mg/min$ | | $\mu l/mg/min$ | nM | $pmol/mg$ |
| Xenotech | 113 (63–163) | 92 (55–128) | 0.81 | 0.17 (0.14–0.21) | 26.7 (17.2–36.2) | |
| HLM141 | 149 (102–210) | 356 (237–475) | 2.39 | 0.63 (0.5–0.8) | 12.9 (7.5–18.4) | 40 |
| HLM146 | 178 (98–258) | 115 (63–166) | 0.64 | 0.09 (0.04–0.13) | 8.3 (2.0–14.7) | 10 |
| HLM148 | 114 (59–179) | 156 (101–211) | 1.37 | 0.15 (0.12–0.18) | 11.2 (6.5–15.9) | 10 |
| HLM153 | 98 (67–130) | 89 (64–114) | 0.91 | 0.16 (0.13–0.19) | 7.9 (5.2–10.7) | |
| Mean \pm S.D. | 130 \pm 33 | 161 \pm 112 | 1.2 \pm 0.7 | 0.21 \pm 0.22 | 13.4 \pm 7.7 | |

^a $E_1 = V_{max1}/K_{m1}$.

^b Data were previously reported by Madani et al. (1999).

CYP3A4 and CYP3A5. The kinetic experiments were performed with and without cytochrome b_5 supplementation (3:1 cytochrome b_5 to P450) to examine the effect of this electron donor on the CYP3A-mediated reaction.

N-Demethylation of oxycodone by CYP3A4 exhibited a typical hyperbolic profile, whereas CYP3A5-catalyzed noroxycodone formation did not reach apparent saturation up to a substrate concentration of 750 μM . Kinetic modeling using a uni-enzyme Michaelis-Menten model (eq. 1) yielded estimates for CYP3A4 noroxycodone formation with and without cytochrome b_5 supplementation (Table 3). Upon supplementation of cytochrome b_5 , increases in K_m (2-fold) and k_{cat} (5-fold) were observed; intrinsic clearance increased by 2.6-fold. The K_m for CYP3A4 *N*-demethylation in the presence of cytochrome b_5 supplementation was closer to the observed K_m for CYP3A-mediated oxycodone *N*-demethylation in liver microsomes.

Similar to CYP3A4, addition of cytochrome b_5 increased oxycodone CYP3A5 intrinsic clearance by more than 2-fold. The apparent lack of saturation over the substrate concentration range suggests that K_m for CYP3A5-mediated oxycodone *N*-demethylation is in the millimolar range. The intrinsic clearance estimated from the slope of the linear portion of the velocity versus substrate concentration plot (<200 μM) exceeded that of CYP3A4 by 33% and 22% in the respective absence and presence of cytochrome b_5 . There was a reasonably good prediction of V_{max} for microsomes from each of the human livers based on the cytochrome b_5 -supplemented Supersome CYP3A4 and CYP3A5 turnover data and the specific content of CYP3A4 and CYP3A5.

O-Demethylation of oxycodone and noroxycodone by CYP2D6*1 Supersomes was examined. This preparation of recombinant CYP2D6 contained coexpressed cytochrome b_5 and cytochrome P450 reductase. Hyperbolic saturation plots were observed for both oxycodone and noroxycodone (Fig. 6). The K_m for Supersome CYP2D6-mediated oxycodone *O*-demethylation was on average 3-fold lower than the K_m in human liver microsomes. CYP2D6 Supersomes efficiently catalyzed the *O*-demethylation of noroxycodone to noroxymorphone. K_m for CYP2D6-mediated noroxycodone *O*-demethylation was 2-fold lower, and V_{max} was 20% higher than 2D6-mediated oxycodone *O*-demethylation; hence, intrinsic clearance for *O*-demethylation of noroxycodone was 2.5-fold higher than that of oxycodone (Table 3).

Discussion

The role of P450 enzymes in the metabolism of weak oral opioids has attracted significant attention since the early 1990s when it was

recognized that CYP2D6 catalyzes *O*-demethylation of codeine to morphine and is a major determinant of its analgesic efficacy. However, follow-up studies with other 3- and 17-methylated morphine analogs failed to show a similar pharmacodynamic importance of CYP2D6-mediated *O*-demethylation as with codeine (vide infra). Attention has recently shifted to the other phase I metabolic pathways of these opioids with respect to their potential role in opioid pharmacodynamics, vis-à-vis active metabolite formation.

We undertook the present study to identify the major P450 enzymes responsible for oxycodone *N*-demethylation to noroxycodone and *O*-demethylation to oxymorphone, and to assess their relative contribution to the oxidative metabolism of oxycodone using human liver and intestinal microsomes.

N-Demethylation of oxycodone to noroxycodone represents the predominant oxidative pathway in human liver microsomes and was almost exclusively (>90%) catalyzed by CYP3A. For the minor *O*-demethylation pathway, CYP2D6 accounted for 79 to 90% of total intrinsic clearance for oxymorphone formation in the five preparations of human liver microsomes. In the present panel of human liver microsomes, the intrinsic clearance for CYP3A-mediated *N*-demethylation was 2 to 14 times the intrinsic clearance for the parallel CYP2D6-mediated *O*-demethylation; mean intrinsic clearance for noroxycodone formation was 10.5 $\mu l/min/mg$ versus 1.5 $\mu l/min/mg$ for oxymorphone formation. This is consistent with the data from experiments performed with cDNA-expressed enzymes, which showed a 6-fold higher specific activity of CYP3A4-mediated *N*-demethylation versus CYP2D6-mediated *O*-demethylation. Scale-up of our in vitro, microsomal intrinsic clearance values (excluding the data from CYP3A-deficient HLM 146) predicted an in vivo hepatic clearance that was in excellent agreement with the i.v. oxycodone clearance (i.e., within 80–112% of the reported value of 0.78 l/min) (Poyhia et al., 1991). In the human intestinal microsomes, oxycodone oxidation occurred at a much lower rate than that in the human liver microsomes. Assuming a 2- to 5-fold lower *N*-demethylation intrinsic clearance in the intestinal mucosa, the first-pass intestinal extraction is predicted to be ~2%, negligible compared with a predicted liver extraction of 23%.

A high interliver variation in microsomal *N*-demethylation of oxycodone was noted. Genetic polymorphism in the expression of CYP3A5 has recently been recognized as a major contributing factor to the well recognized intersubject variability of CYP3A activity in vivo (Lamba et al., 2002; Lin et al., 2002). This led us to investigate the comparative oxidative activity of recombinant CYP3A4 and CYP3A5 toward oxycodone. The intrinsic clearance of CYP3A5 was

TABLE 3

Estimates of Michaelis-Menten parameters for oxycodone metabolite formation in Gentest Supersomes containing recombinant CYP3A4, CYP3A5, and CYP2D6

k_{cat} is defined as V_{max} per mole of expressed enzyme. Values in parentheses represent the 95% confidence intervals of the regression estimates.

| Reaction | P450 | K_m μM | k_{cat} 1/min | CL_{int} $\mu l/min/pmol$ P450 |
|-------------------------------------|-------------|---------------------|-----------------------|-------------------------------------|
| Oxycodone→Noroxycodone | 3A4 | 377 (235–519) | 4.7 (3.78–5.57) | 0.012 |
| | 3A4 + b_5 | 670 (595–744) | 21.7 (20.28–23.14) | 0.032 |
| Oxycodone→Noroxycodone ^a | 3A5 | | | 0.017 |
| Oxycodone ^b →Oxymorphone | 3A5 + b_5 | | | 0.040 |
| | 2D6*1 | 39.8 (31.0–48.7) | 11.4 (10.8–12.0) | 0.286 |
| Noroxycodone→Noroxymorphone | 2D6*1 | 20.5 (15.2–25.9) | 14.9 (14.1–15.7) | 0.727 |

^a CYP3A5-mediated formation of noroxycodone did not reach apparent saturation within the substrate concentration used.

^b Two-fold difference between the oxycodone K_m in HLM and Supersomes has been noted and may be attributed to variable levels of cytochrome P450 reductase (OR) present in Gentest Supersomes.

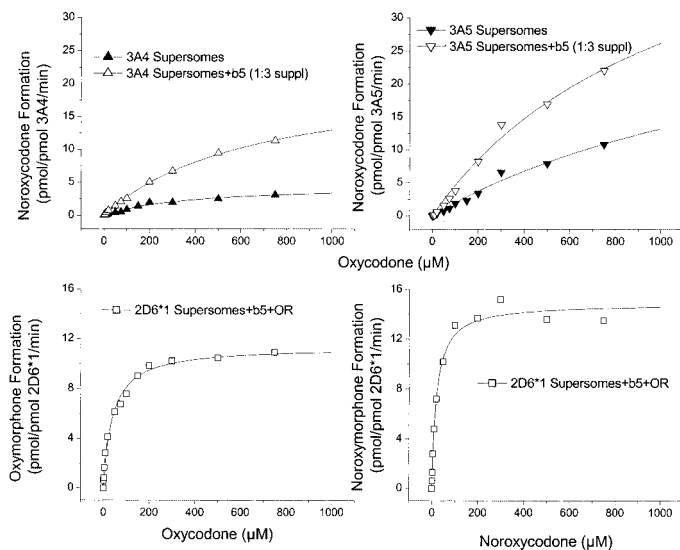


FIG. 6. Formation kinetics of noroxycodone, oxymorphone, and noroxymorphone in Gentest Supersomes.

The upper panels show the formation kinetics of noroxycodone by Gentest Supersomes CYP3A4 and CYP3A5 with or without cytochrome b_5 supplementation. The lower panels show the formation kinetics of oxymorphone from oxycodone (left) and noroxymorphone from noroxycodone (right) by Gentest Supersomes CYP2D6.

comparable with that of CYP3A4. CYP3A5 expression could explain the between-liver variability in oxycodone *N*-demethylation. Indeed, there was a rank order correlation of *N*-demethylation intrinsic clearance with the sum of CYP3A4 and CYP3A5 content. It is interesting to note that HLM 141, which has the highest content of CYP3A5 in our human liver bank, exhibited the highest intrinsic clearance for oxycodone *N*-demethylation.

The present K_m estimates for noroxycodone and oxymorphone formation from oxycodone are lower than values reported in a recent abstract by Somogyi (1999). The abstract reported a mean K_m for oxycodone *N*-demethylation of 1.6 ± 0.2 mM, compared with our 600 ± 119 μM ; V_{max} values were similar to those from this study. It was mentioned that ketoconazole and CYP3A4 antibody were able to inhibit noroxycodone formation completely, which is consistent with our present finding with ketoconazole. The abstract further reported a mean K_m of 262 ± 81 μM for oxycodone *O*-demethylation by liver microsomes from four “extensive metabolizers” of CYP2D6, which is 2-fold higher than our K_m estimate of 130 ± 33 μM . The K_m for

microsomes from one “poor metabolizer” (PM) was even higher at 924 μM . V_{max} was reported at 135 ± 22 pmol/mg/min for the extensive metabolizer microsomes and 49 pmol/mg/min for the PM microsomal (Somogyi, 1999); the former value is reasonably similar to our present estimate of 161 ± 112 pmol/mg/min. None of the human livers in our study carry the common CYP2D6 PM genotype.

The differences in K_m estimates between the two studies may be related to the difficulty in resolving the multienzyme kinetics of P450-mediated oxycodone oxidation. Initial enzyme kinetic modeling of velocity data, in the absence of inhibitors, failed to conclusively discriminate between uni- and multienzyme models. We refined our experimental approach to include incubations with CYP3A- and CYP2D6-specific inhibitors, i.e., ketoconazole and quinidine. This design allowed a definitive assignment of the high affinity catalytic component of oxycodone *N*-demethylation to CYP3A and that of *O*-demethylation to CYP2D6. Although the inclusion of the inhibition data requires estimation of an additional K_i term, the model parameters were estimated with greater precision due to the additional information.

The experiment with lymphoblast microsomes expressing individual P450s suggested that, aside from CYP3A and CYP2D6, other P450 enzymes (e.g., CYP2C19) may be involved in the formation of both noroxycodone and oxymorphone. Quantitative contribution of these other isoforms appears to be minor, at least at their constitutive level of expression.

Our *in vitro* findings are consistent with available *in vivo* data from pharmacokinetic studies in human volunteers and patients. Very low (<2 ng/ml) circulating concentrations of oxymorphone have been observed following a single oral dose of oxycodone; the AUC ratios oxymorphone to parent drug were <0.01. On the other hand, plasma noroxycodone concentrations were reported to be significantly higher and comparable with the parent drug; noroxycodone to parent AUC ratios were slightly above unity (Poyhia et al., 1991, 1992; Kaiko et al., 1996; Heiskanen et al., 1998). A low presence of circulating oxymorphone could either be explained by its limited formation or efficient clearance (i.e., 3-*O*-glucuronidation). On the other hand, the high circulating concentration of noroxycodone could be attributed to either extensive *N*-demethylation of oxycodone or a slow clearance of noroxycodone. The present microsomal data point to a very limited extent of *O*-demethylation, while clearly establishing *N*-demethylation as a major primary pathway in oxycodone metabolism.

Studies to date suggest a minor role of oxymorphone in the pharmacodynamics of oxycodone. Cleary et al. (1994) examined the effect of quinine pretreatment (potent inhibition of CYP2D1) on the antinociceptive effect of oxycodone in Sprague-Dawley rats. No attenuation of

antinociception was observed with quinine pretreatment. Heiskanen et al. (1998) investigated the effects of CYP2D6 inhibition by quinidine on the side-effects of slow release oxycodone in 10 healthy human volunteers, who were extensive metabolizers of CYP2D6. There was no change in the subjective or psychomotor effects of oxycodone following cotreatment with quinidine as compared with placebo, despite a dramatic decrease in plasma oxymorphone due to inhibition of CYP2D6.

These available oxycodone pharmacodynamic data do not follow the recognized importance of CYP2D6-mediated activation in codeine pharmacology but are consistent with findings from other structurally related 6-keto oral opioids in terms of the limited impact of CYP2D6-generated metabolites on their opioid-related effects. CYP2D6 inhibition studies with hydrocodone or dihydrocodeine have all failed to demonstrate any significant impact on subjective opioid response in human subjects (Kaplan et al., 1997) or antinociception in rats (Tomkins et al., 1997; Wilder-Smith et al., 1998).

The prominence of *N*-demethylation in oxycodone metabolism raises the possibility that this pathway may be a source of active metabolites that contribute to the pharmacodynamics of oxycodone. As mentioned earlier, noroxycodone is an active opioid, albeit modest in antinociceptive activity (Leow and Smith, 1994). Nonetheless, its relatively high circulating concentration following oral administration of oxycodone in human subjects warrants consideration. Noroxymorphone, which is shown in the present study to derive mainly from *O*-demethylation of noroxycodone, could be an important active metabolite. We recently examined the affinity of oxycodone metabolites for a cloned human μ -opioid peptide receptor (data to be published). Noroxymorphone demonstrated 3- and 10-fold higher affinity than oxycodone and noroxycodone, respectively. Chen et al. (1991) have also reported a 2-fold higher noroxymorphone binding affinity for μ -receptor in rat brain homogenates over oxycodone. Further in vivo studies will be required to ascertain whether noroxycodone, noroxymorphone, and any other metabolites derived from the *N*-demethylation pathway have a significant role in the pharmacodynamics of oxycodone.

In summary, our study offers a full elucidation of oxycodone oxidation by human liver P450 enzymes. We identified CYP3A4 to be the principal *N*-demethylase and CYP2D6 the major *O*-demethylase of oxycodone in human liver microsomes. *N*-Demethylation is the major oxidative pathway; hence, CYP3A expression and activity are expected to be a major determinant of oxycodone clearance in vivo, e.g., polymorphic expression of CYP3A5. Our finding of a limited extent of CYP2D6-mediated *O*-demethylation is consistent with the previously reported low circulating concentration of oxymorphone following oral oxycodone administration in human subjects, which explains its apparent lack of contribution to the pharmacodynamics of oxycodone. Finally, the active secondary oxidative metabolite, noroxymorphone, is shown to be an *O*-demethylation product of noroxycodone and may have an important role in the pharmacodynamics of oxycodone.

References

Caraco Y, Sheller J, and Wood AJ (1996a) Pharmacogenetic determination of the effects of codeine and prediction of drug interactions. *J Pharmacol Exp Ther* **278**:1165–1174.
 Caraco Y, Tateishi T, Guengerich FP, and Wood AJ (1996b) Microsomal codeine *N*-demethylation: cosegregation with cytochrome P4503A4 activity. *Drug Metab Dispos* **24**:761–764.
 Chen ZR, Irvine RJ, Somogyi AA, and Bochner F (1991) Mu receptor binding of some commonly used opioids and their metabolites. *Life Sci* **48**:2165–2171.
 Childers SR, Creese I, Snowman AM, and Snyder SH (1979) Opiate receptor binding affected differentially by opiates and opioid peptides. *Eur J Pharmacol* **55**:11–18.
 Cleary J, Mikus G, Somogyi A, and Bochner F (1994) The influence of pharmacogenetics on opioid analgesia: studies with codeine and oxycodone in the Sprague-Dawley/Dark Agouti rat model. *J Pharmacol Exp Ther* **271**:1528–1534.
 Curtis GB, Johnson GH, Clark P, Taylor R, Brown J, O'Callaghan R, Shi M, and Lacouture PG

(1999) Relative potency of controlled-release oxycodone and controlled-release morphine in a postoperative pain model. *Eur J Clin Pharmacol* **55**:425–429.
 Dayer P, Desmeules J, Leemann T, and Striberni R (1988) Bioactivation of the narcotic drug codeine in human liver is mediated by the polymorphic monooxygenase catalyzing debrisoquine 4-hydroxylation (cytochrome P-450 db1/buff). *Biochem Biophys Res Commun* **152**:411–416.
 Dayer P, Leemann T, and Striberni R (1989) Dextromethorphan *O*-demethylation in liver microsomes as a prototype reaction to monitor cytochrome P-450 db1 activity. *Clin Pharmacol Ther* **45**:34–40.
 De Conno F, Ripamonti C, Sbanotto A, Barletta L, Zecca E, Martini C, and Ventafridda V (1991) A clinical study on the use of codeine, oxycodone, dextropropoxyphene, buprenorphine and pentazocine in cancer pain. *J Pain Symptom Manage* **6**:423–427.
 Gibbs MA, Thummel KE, Shen DD, and Kunze KL (1999) Inhibition of cytochrome P-450 3A (CYP3A) in human intestinal and liver microsomes: comparison of K_i values and impact of CYP3A5 expression. *Drug Metab Dispos* **27**:180–187.
 Glare PA and Walsh TD (1993) Dose-ranging study of oxycodone for chronic pain in advanced cancer. *J Clin Oncol* **11**:973–978.
 Gorski JC, Jones DR, Wrighton SA, and Hall SD (1994) Characterization of dextromethorphan *N*-demethylation by human liver microsomes. Contribution of the cytochrome P450 3A (CYP3A) subfamily. *Biochem Pharmacol* **48**:173–182.
 Heiskanen T, Olkkola KT, and Kalso E (1998) Effects of blocking CYP2D6 on the pharmacokinetics and pharmacodynamics of oxycodone. *Clin Pharmacol Ther* **64**:603–611.
 Ishida T, Oguri K, and Yoshimura H (1979) Isolation and identification of urinary metabolites of oxycodone in rabbits. *Drug Metab Dispos* **7**:162–165.
 Ishida T, Oguri K, and Yoshimura H (1982) Determination of oxycodone metabolites in urines and feces of several mammalian species. *J Pharmacobiodyn* **5**:521–525.
 Kaiko RF, Benziger DP, Fitzmartin RD, Burke BE, Reder RF, and Goldenheim PD (1996) Pharmacokinetic-pharmacodynamic relationships of controlled-release oxycodone. *Clin Pharmacol Ther* **59**:52–61.
 Kaplan HL, Busto UE, Baylon GJ, Cheung SW, Otton SV, Somer G, and Sellers EM (1997) Inhibition of cytochrome P450 2D6 metabolism of hydrocodone to hydromorphone does not importantly affect abuse liability. *J Pharmacol Exp Ther* **281**:103–108.
 Kirvela M, Lindgren L, Seppala T, and Olkkola KT (1996) The pharmacokinetics of oxycodone in uremic patients undergoing renal transplantation. *J Clin Anesth* **8**:13–18.
 Kronbach T, Mathys D, Gut J, Catin T, and Meyer UA (1987) High-performance liquid chromatographic assays for buprenorphin 3'-hydroxylase, debrisoquine 4-hydroxylase and dextromethorphan *O*-demethylase in microsomes and purified cytochrome P-450 isozymes of human liver. *Anal Biochem* **162**:24–32.
 Lamba JK, Lin YS, Schuetz EG, and Thummel KE (2002) Genetic contribution to variable human CYP3A-mediated metabolism. *Adv Drug Deliv Rev* **54**:1271–1294.
 Leow KP and Smith MT (1994) The antinociceptive potencies of oxycodone, noroxycodone and morphine after intracerebroventricular administration to rats. *Life Sci* **54**:1229–1236.
 Lin YS, Dowling AL, Quigley SD, Farin FM, Zhang J, Lamba J, Schuetz EG, and Thummel KE (2002) Co-regulation of CYP3A4 and CYP3A5 and contribution to hepatic and intestinal midazolam metabolism. *Mol Pharmacol* **62**:162–172.
 Madani S, Paine MF, Lewis L, Thummel KE, and Shen DD (1999) Comparison of CYP2D6 content and metoprolol oxidation between microsomes isolated from human livers and small intestines. *Pharm Res (NY)* **16**:1199–1205.
 Melmon KL, Hoffman BB, and Niernberg DW (2000) *Melmon and Morelli's Clinical Pharmacology*. McGraw-Hill, New York.
 Nuutinen LS, Wuolijoki E, and Pentikainen IT (1986) Diclofenac and oxycodone in treatment of postoperative pain: a double-blind trial. *Acta Anaesthesiol Scand* **30**:620–624.
 Obach RS (1999) Prediction of human clearance of twenty-nine drugs from hepatic microsomal intrinsic clearance data: an examination of in vitro half-life approach and nonspecific binding to microsomes. *Drug Metab Dispos* **27**:1350–1359.
 Otton SV, Wu D, Joffe RT, Cheung SW, and Sellers EM (1993) Inhibition by fluoxetine of cytochrome P450 2D6 activity. *Clin Pharmacol Ther* **53**:401–409.
 Parris WC, Johnson BW Jr, Croghan MK, Moore MR, Khojasteh A, Reder RF, Kaiko RF, and Buckley BJ (1998) The use of controlled-release oxycodone for the treatment of chronic cancer pain: a randomized, double-blind study. *J Pain Symptom Manage* **16**:205–211.
 Poulsen L, Brosen K, Arendt-Nielsen L, Gram LF, Elbaek K, and Sindrup SH (1996) Codeine and morphine in extensive and poor metabolizers of sparteine: pharmacokinetics, analgesic effect and side effects. *Eur J Clin Pharmacol* **51**:289–295.
 Poyhia R, Olkkola KT, Seppala T, and Kalso E (1991) The pharmacokinetics of oxycodone after intravenous injection in adults. *Br J Clin Pharmacol* **32**:516–518.
 Poyhia R, Seppala T, Olkkola KT, and Kalso E (1992) The pharmacokinetics and metabolism of oxycodone after intramuscular and oral administration to healthy subjects. *Br J Clin Pharmacol* **33**:617–621.
 Segel I (1975) *Enzyme Kinetics*, John Wiley & Sons, New York.
 Silvasti M, Rosenberg P, Seppala T, Svartling N, and Pitkanen M (1998) Comparison of analgesic efficacy of oxycodone and morphine in postoperative intravenous patient-controlled analgesia. *Acta Anaesthesiol Scand* **42**:576–580.
 Sindrup SH and Jensen TS (1999) Efficacy of pharmacological treatments of neuropathic pain: an update and effect related to mechanism of drug action. *Pain* **83**:389–400.
 Somogyi AA (1999) Characterization of cytochrome P450 informants involved in oxycodone oxidative metabolism in humans, in *9th World Congress on Pain*; 1999 Aug 23–27; Vienna, Austria.
 Tomkins DM, Otton SV, Joharchi N, Li NY, Balster RF, Tyndale RF, and Sellers EM (1997) Effect of cytochrome P450 2D1 inhibition on hydrocodone metabolism and its behavioral consequences in rats. *J Pharmacol Exp Ther* **280**:1374–1382.
 Watson CP and Babul N (1998) Efficacy of oxycodone in neuropathic pain: a randomized trial in postherpetic neuralgia. *Neurology* **50**:1837–1841.
 Weinstein SH and Gaylor JC (1979) Determination of oxycodone in plasma and identification of a major metabolite. *J Pharm Sci* **68**:527–528.
 Wilder-Smith CH, Hufschmid E, and Thormann W (1998) The visceral and somatic antinociceptive effects of dihydrocodeine and its metabolite, dihydromorphine. A cross-over study with extensive and quinidine-induced poor metabolizers. *Br J Clin Pharmacol* **45**:575–581.